Hepatic uptake of β-VLDL in cholesterol-fed rabbits

Ola Gudmundsen,[1] Trond Berg, Norbert Roos,* and Marit S. Nenseter†

Department of Molecular Cell Biology and Department of Electron Microscopy,* Institute of Biology, University of Oslo, P.O. Boxes 1050 and 1066,* Blindern, N-0316 Oslo, Norway; and Institute for Nutrition Research,† University of Oslo, P.O. Box 1046, Blindern, N-0316 Oslo, Norway

Abstract The hepatic uptake of intravenously injected β-very low density lipoprotein (β-VLDL) in rabbits fed 2% (w/w) cholesterol for 3 weeks was investigated. In vitro studies were also conducted to examine the specificity and the capacity of the uptake in isolated liver parenchymal cells. The hepatic uptake of β-VLDL was 15.8 ± 6.7% (n = 6) in the cholesterol-fed rabbits as compared to 26.6 ± 7.5% (n = 6) of the injected dose in control rabbits ($P < 0.05$). Although this is a fractional reduction, it represents a more than 10-fold increase in absolute hepatic uptake of lipoproteins in the cholesterol-fed rabbits. In these animals the liver parenchymal, endothelial, and Kupffer cells took up 10.2 ± 2.7%, 3.0 ± 0.9%, and 1.8 ± 0.4% of the injected dose, respectively, compared to 25.9 ± 6.1%, 3.6 ± 1.6%, and 1.5 ± 0.8% of the injected dose in chow-fed controls. However, taking into account the high plasma lipoprotein levels in the cholesterol-fed rabbits, the absolute cellular uptake was 10-fold increased in the parenchymal liver cells and more than 20-fold increased in the nonparenchymal cells. In vitro results indicated a 40% down-regulation of the specific receptor for β-VLDL in the parenchymal cells, and this, together with an increased competition for binding sites in the hypercholesterolemic rabbits, probably explains the reduced uptake of β-VLDL in terms of % of injected dose observed in vivo. In vitro data suggested that the receptor involved in both hypercholesterolemic and normolipemic rabbits was the apolipoprotein (apo) B,E receptor. On a per cell basis, parenchymal cells from chow-fed control animals took up 2.4 ± 0.8% of the injected dose per 10^9 cells; this uptake was reduced to 1.1 ± 0.5% in hypercholesterolemic animals. No differences in uptake of β-VLDL in nonparenchymal liver cells were observed on a per cell basis between the two feeding groups, indicating that binding sites involved in this uptake are not down-regulated by cholesterol feeding. On the contrary, the absolute uptake in the nonparenchymal liver cells is greatly increased in hypercholesterolemic rabbits as compared to controls. In cholesterol-fed rabbits the three different liver cell types took up approximately the same amount of β-VLDL per cell. The liver nonparenchymal cells, therefore, assume a prominent role in uptake of β-VLDL in hypercholesterolemic rabbits, accounting for more than 30% of the total hepatic uptake as compared to 16% in control animals. Electron microscopic studies showed a significant accumulation of lipids in all cell types investigated from cholesterol-fed rabbits, while no such lipid accretion could be observed in control rabbits. The in vivo data show that the nonparenchymal cells, notably the Kupffer cells, play an important role in catabolizing β-VLDL in hypercholesterolemic rabbits.—**Gudmundsen, O., T. Berg, N. Roos, and M. S. Nenseter.** Hepatic uptake of β-VLDL in cholesterol-fed rabbits. *J. Lipid Res.* 1993. **34:** 589–600.

Supplementary key words liver parenchymal cells • Kupffer cells • liver endothelial cells • plasma clearance • hypercholesterolemic rabbits

Feeding rabbits diets high in cholesterol causes marked alterations in the plasma lipoproteins. One of these changes is the appearance of β-VLDL. β-VLDL are cholesterol-enriched lipoproteins that contain apoB and apoE as their major protein constituents. β-VLDL is also produced in patients with type III hyperlipidemia (1, 2). Cholesterol-rich β-VLDL has been shown to cause cholesteryl ester accumulation in macrophages (3), similar to that seen after uptake of chemically modified low density lipoprotein (LDL) mediated by the scavenger receptor. It might also induce monocyte adhesion to endothelial cells (4). β-VLDL may accumulate in aorta and atherosclerotic lesions (5, 6), and this lipoprotein has therefore been considered to have a potential role in development of atherosclerosis. Although macrophages take up β-VLDL avidly, the liver is the main organ of β-VLDL catabolism (7–10). Yet, the role of the different liver cell types in the uptake of β-VLDL in hypercholesterolemic animals has not been investigated.

The functional units of the mammalian liver are hexagonally shaped lobuli consisting of many layers of platelets of parenchymal cells. The sinusoids, which are specialized capillaries, bring both venous blood from the digestive system and arterial blood through the lobuli. The sinusoids are lined with the endothelial cells that separate the sinusoidal lumen from the space of Disse and the underlying parenchymal cells. The endothelial cells often cover the whole circumference of a sinusoid. They display 100-nm fenestrations that allow free passage of macromolecules and lipoproteins (except chylomicrons)

Abbreviations: apo, apolipoprotein; β-VLDL, β-very low density lipoprotein; LDL, low density lipoprotein; LDL(cr), cholesterol-rich low density lipoprotein; TC, tyramine cellobiose; PBS, phosphate-buffered saline; FCR, fractional catabolic rate; ACR, absolute catabolic rate.

[1]To whom correspondence should be addressed.

to the space of Disse (11). Within the sheets of parenchymal cells are bile canaliculi that transport bile to the bile ducts. The Kupffer cells, the liver macrophages, are usually observed in the lumen of the sinusoid.

In normolipidemic rats, β-VLDL is taken up mainly by parenchymal liver cells; however, contrary to expectations, rat Kupffer cells do not take up significant amounts of β-VLDL (8). In rat liver a relatively high proportion of the apoB,E receptor is located in the Kupffer cells. The rat liver parenchymal cells express relatively low levels of the apoB,E receptor. Thus, in this respect the liver macrophages behave differently from other types of macrophages which avidly take up β-VLDL via an apoB,E receptor (12). The finding that the β-VLDL is taken up exclusively by the parenchymal liver cells, therefore, suggests that β-VLDL uptake is mediated via an apoB,E receptor-independent mechanism in rats (13). In the present investigation rabbits were used, because lipoprotein metabolism in rabbits resembles that of humans, in that the plasma concentrations of LDL are relatively high and the liver expresses high levels of the apoB,E receptor (14, 15). β-VLDL has high affinity for the apoB,E receptor (16) and mRNA for this receptor has been identified in liver parenchymal, endothelial, and Kupffer cells in cholesterol-fed rabbits as well as chow-fed controls (14, 17).

Our objectives were: *i)* to determine the contribution of different cell types to the hepatic uptake of β-VLDL; *ii)* to investigate the effect of cholesterol feeding on the morphology of each liver cell type by transmission electron microscopy; and *iii)* to determine the specificity of the receptors involved in the in vitro uptake of β-VLDL in liver parenchymal cells from cholesterol-fed and control-fed rabbits. The results obtained were compared with those previously found for the hepatic uptake of cholesterol-rich LDL (LDL(cr)) (17).

EXPERIMENTAL

Experimental animals and diets

Male Chinchilla rabbits, weighing 2–3 kg, obtained from GMBH Versuchtierkunde und Zucht, Germany, were used in all experiments. One group of animals was fed a 2% (w/w) cholesterol chow (EWOS Maintenance Feed) for 3 weeks (n = 6). The control group received ordinary laboratory chow (n = 6). Both groups were fed ad libitum. In the control group, plasma levels of cholesterol, triacylglycerols, and phospholipids were 3.2 ± 0.2 mmol/l, 1.7 ± 0.2 mmol/l, and 6.4 ± 1.0 mmol/l, respectively, compared to 39 ± 8.6 mmol/l, 1.7 ± 0.2 mmol/l, and 8.4 ± 2.9 mmol/l, respectively, in the cholesterol-fed group.

Chemicals and assays

Bovine serum albumin and collagenase (type I) were purchased from Sigma Chemical Co., St. Louis, MO. $Na^{125}I$ and $Na^{131}I$ were obtained from The Radiochemical Centre, Amersham, Bucks., UK. Tyramine cellobiose-adduct was a kind gift from Dr. Helge Tolleshaug, Nycomed A/S, Oslo, Norway. All other chemicals and solvents were high-purity commercial materials.

Triacylglycerols were measured enzymatically by Nycotest kits (Nycomed A/S, Oslo, Norway). Free and esterified cholesterol and phospholipids were measured enzymatically with kits from Bio Mérieux, Marcy-l'Etiole, France. Cholesterol and cholesteryl ester in cultured cells were determined by Folchs extraction (18) followed by gas–liquid chromatography with a 6 ft, 2 mm capillary column on a Schimadzu GC-14A chromatograph at 295°C. Protein was determined with a BCA protein assay obtained from Pierce Europe B.V., Oud-Beijerland, The Netherlands, with bovine serum albumin as standard. SDS polyacrylamide gel electrophoresis was performed according to Laemmli (19). The gels were stained with Coomassie blue and radioactivity in apolipoprotein bands was measured by autoradiography; the relative distribution was determined by densitometry, as described by Nenseter et al. (20).

Lipoproteins

β-VLDL and LDL(cr) were isolated from fresh, pooled rabbit plasma after 2 weeks of cholesterol feeding and 14 h fasting. Lipoproteins were separated by sequential flotational ultracentrifugation in a Centrikon T-2060 with a TFT 70.38 rotor for 20 h at 40,000 rpm at 10°C (21). Density ranges of < 1.006 g/ml and 1.019–1.063 g/ml for β-VLDL and LDL(cr) were used, respectively. β-VLDL was radiolabeled with ^{131}I-labeled tyramine cellobiose(TC) and LDL(cr) with ^{125}I-labeled TC (22). Tyramine cellobiose traps the label in the organelle in which degradation takes place. The labeled lipoproteins were dialyzed against 0.15 M NaCl, 20 mM sodium phosphate, and 1 mM EDTA, pH 7.4. More than 97% of the radioactivity was precipitated by 10% (w/v) trichloroacetic acid. The specific radioactivities were 9 and 176 cpm/ng protein for ^{131}I-labeled TC-β-VLDL and 50 and 355 cpm/ng protein for ^{125}I-labeled TC-LDL(cr). In the ^{131}I-labeled TC-β-VLDL, apoB contained 27% and apoE 51% of the total radioactivity, whereas in the ^{125}I-labeled TC-LDL(cr), the apoB contained 82% and apoE contained 16% of the total radioactivity. The percent (w/w) distributions of total cholesterol, triacylglycerols, phospholipids, and proteins in the lipoproteins were 65.1, 3.1, 22.0, and 9.8, respectively, for β-VLDL and 61.1, 3.0, 13.2, and 22.7, respectively, for LDL(cr) (n = 2) (pooled plasma from three

rabbits). The particle sizes were 59.0 ± 21.6 nm and 30.1 ± 2.9 nm (n = 4) for β-VLDL and LDL(cr), respectively, determined by dynamic light scattering/photon correlation spectroscopy using 54.5 nm latex particles as standards (23). Results obtained by negative stain measurements gave slightly smaller lipoprotein sizes (53 ± 17 nm (n = 21) and 24 ± 4 (n = 16) for β-VLDL and LDL(cr), respectively). This may be due to shrinking because samples were measured in a dehydrated environment in contrast to photon correlation spectroscopy. Human LDL and LDL from control-fed rabbits were isolated as described above for LDL(cr).

In vivo studies

After 3 weeks of cholesterol feeding, the rabbits were injected with ^{131}I-labeled TC-β-VLDL into the marginal ear vein. To detect a possible down-regulation of the hepatic uptake of the lipoproteins control-fed rabbits were also injected. ^{125}I-labeled TC-LDL(cr) was also injected simultaneously in both animal groups for comparison. Blood samples (100 μl) were drawn from the opposite ear at 5 and 30 min and 1, 2, 3, 4, 5, 6, 7, and 24 h after injection. The radioactivity in the blood samples was counted in a Kontron Automatic Gamma Counter MB252. The radioactivity in whole plasma volume was calculated by assuming plasma to be 3.28% of the total body weight (24). Data were fitted to biexponential decay equations, and fractional catabolic rates (FCR) (25) were calculated from the second (β) linear phase using Sigmaplot software (Sigma Co., St Louis, MO). Absolute catabolic rates (ACR) were calculated by multiplying these rates by the plasma apolipoprotein pool sizes.

After 24 h, between 9:00 and 10:00 AM, animals were anesthetized with an intraperitoneal injection of Dormicum (Roche), 0.5 ml/kg and 5 min later by an intramuscular injection of Hypnorm (Janssen), 0.4 ml/kg. A small liver lobe was tied off after 5 min of in situ perfusion with a Ca^{2+}-free buffer for determination of total radioactivity in the liver. Liver cell suspensions were obtained by enzymatic perfusion of the liver (26, 27) by a two-step procedure (28) with a flow rate of 100 ml/min. The liver cell suspension was filtered through nylon gauze, and the parenchymal cells were sedimented by centrifugation for 2 min at 20 *g*. The pellet was resuspended in incubation buffer (29) and the centrifugation was repeated. Nonparenchymal liver cells were sedimented from the resulting supernatant by centrifugation for 4 min at 310 *g*. Parenchymal and nonparenchymal cells were further purified by centrifugal elutriation using a Beckman JE-6 rotor and J-21 centrifuge. Hepatocytes were elutriated at 1200 rev/min at flow rate 25–50 ml/min and nonparenchymal cells were elutriated at 1500 rev/min at flow rate 25 ml/min. The parenchymal cells were free of contaminating nonparenchymal cells and vice versa, as characterized by their different size. The cells were then washed in RPMI 1640 medium. Hepatocytes were seeded on fibronectin-coated dishes in RPMI 1640, whereas pure endothelial and Kupffer cells were prepared from the nonparenchymal cells by a selective attachment method, previously described by Laakso and Smedsrød (30). In short, the nonparenchymal cells were first seeded on bovine serum albumin/glutaraldehyde-pretreated dishes. After 20 min of incubation, the Kupffer cells had attached. Nonattached cells were then seeded on fibronectin-coated dishes. Kupffer and endothelial cell cultures were more than 95% pure as judged by peroxidase staining of the Kupffer cells. All cell cultures were washed after 2 h incubation at 37°C, dissolved in a solution of 0.1% SDS in 0.3 M NaOH, and the radioactivity was counted. The number of cells in each dish were determined by microscopy. A minimum of six fields including more than 500 cells were counted using an ocular network. The calculated standard deviations were all less than 5% of the mean value.

Cellular distributions between liver parenchymal, endothelial, and Kupffer cells of ^{131}I-labeled TC-βVLDL and ^{125}I-labeled TC-LDL(cr) were expressed as a percentage of injected dose per billion cells. To estimate the contribution of each cell type to the total hepatic uptake, the values above were multiplied by the number of each cell type in the whole liver. It was assumed that 1 g of liver contained 125 × 10^6 parenchymal cells, 36 × 10^6 endothelial cells, and 19 × 10^6 Kupffer cells (31, 32). These values refer to rat, because corresponding values for rabbit have not yet been published, to our knowledge. The recoveries of radioactivity in the liver using these values were 84.5 ± 13% and 84.8 ± 18.6% for ^{131}I-labeled TC-βVLDL in cholesterol-fed and normal rabbits, respectively. The liver weight was found to be 3.47 ± 0.38% of body weight (n = 4).

Electron microscopy

Different liver cell types grown on Falcon 3006 optical dishes (60 × 15 mm) and small blocks of liver (1 mm^3) were fixed in a buffer containing 2.5% glutaraldehyde. After glutaraldehyde fixation for 48 h at 4°C, the fixation buffer was replaced by a 0.1 M cacodylate buffer (pH 7.4) and the tissue pieces and cells were washed twice for 10 min at 4°C. The samples were postfixed with 4% OsO_4. After rinsing, the samples were dehydrated in an increasing gradient of ethanol (70%, 90%, 96%, and 100%). The tissue samples were embedded directly in Spurr resin, whereafter a mixture of Spurr resin and 100% ethanol at a ratio 1:2 was added to the dishes for 15 min, replaced by a 1:1 mixture for another 15 min, and finally by 100% Spurr resin. Tissue samples embedded in Spurr resin were polymerized at 70°C for 24 h and at 60°C for 72 h before sections were cut. The dishes were filled with 2–3 mm Spurr resin and beam capsules with their tips cut off were placed on the dishes. After polymerization of the resin at 60°C for 20 h, the capsules were filled with resin

and polymerized at 60°C for 24 h. The beam capsules were broken loose from the petri dish and much of the petri dish material was trimmed away. Fifty-nm sections of both samples were then cut on a LKB III microtome using glass knives. The sections were placed on Formvar/carbon-coated 75-mesh copper grids and stained for 2 min with a saturated uranyl acetate solution in 50% ethanol and for 2 min in 0.2% lead citrate solution in 0.1 N NaOH. The sections were examined using a JEOL 100C and JEOL 100CX transmission electron microscope and an accelerating voltage of 80 kV.

In vitro binding of β-VLDL in rabbit parenchymal liver cells

Crude liver cell suspensions were prepared from cholesterol-fed and control-fed rabbits by collagenase perfusion; parenchymal cells were isolated by means of repeated differential centrifugations and centrifugal elutriation, as described above. The parenchymal cells were resuspended in a 20 mM HEPES buffer, pH 7.5, containing 1% albumin (33) and were more than 95% viable by Trypan blue exclusion test and less than 1% contaminated by nonparenchymal cells. Cell concentration was adjusted to 10^7 cells per ml, and the cells were preincubated for 30 min at 37°C in a shaking water bath.

Cells were incubated for 2 h in Erlenmeyer flasks with ^{125}I-labeled TC-β-VLDL and indicated concentrations of unlabeled lipoproteins. Studies were carried out at 4°C and 37°C, and bound radioactivity was measured in cells centrifuged through dibutylphthalate for 30 sec at 2000 *g*.

Statistical analysis

Mann-Whitney two-sample tests were performed to calculate differences between the groups and the results are presented as means ± standard deviations (SD).

RESULTS

In cholesterol-fed rabbits, β-VLDL has a higher clearance rate than LDL(cr)

Five minutes after injection, plasma levels of ^{131}I-labeled TC-β-VLDL were 98.0 ± 27.3% and 33.2 ± 6.8% of the injected dose in cholesterol-fed and control-fed rabbits, respectively (n = 6 in each group). The corresponding values for ^{125}I-labeled TC-LDL(cr) were 99.8 ± 24.3% and 90.5 ± 7.2% of the injected dose (n = 6). These numbers indicate a very high initial clearance rate for β-VLDL compared to LDL(cr) in control-fed rabbits. However, after the initial 5-min phase, the β-VLDL and LDL(cr) were cleared at comparable, though significantly different ($P < 0.014$), rates in the control animals (**Fig. 1A**). The $T_{1/2}$, ACR and FCR (**Table 1**) show that in cholesterol-fed rabbits both LDL(cr) and β-VLDL were cleared at significantly lower rates than in control rabbits. In the cholesterol-fed rabbits, β-VLDL was cleared more rapidly than LDL(cr) ($P < 0.012$ at 24 h) (Fig. 1B). After 24 h, 35.6 ± 6.2% of injected ^{131}I-labeled TC-β-VLDL and 54.6 ± 5.2% of injected ^{125}I-labeled TC-LDL(cr) were recovered in blood from cholesterol-fed rabbits. The corresponding values for controls were 4.1 ± 0.5% and 9.2 ± 2.2% for β-VLDL and LDL(cr), respectively. Although FCR for β-VLDL was reduced to 35% of the control value, the absolute catabolic rate (ACR) increased. ACR for β-VLDL in control-fed rabbits is very small due to the low plasma level of β-VLDL. Daugherty and colleagues (5) found this flux to be less than 1.1 mg/day. In cholesterol-fed animals, the ACR was calculated to be 25.3 ± 3.8 mg apolipoprotein/day per kg for β-VLDL. According to our data, the theoretical amount of LDL- plus β-VLDL-cholesterol irreversibly cleared from the plasma in a cholesterol-fed rabbit weighing 3 kg will then be 764.5 mg/24 h, where 508.5 mg/24 h is from β-VLDL catabolism.

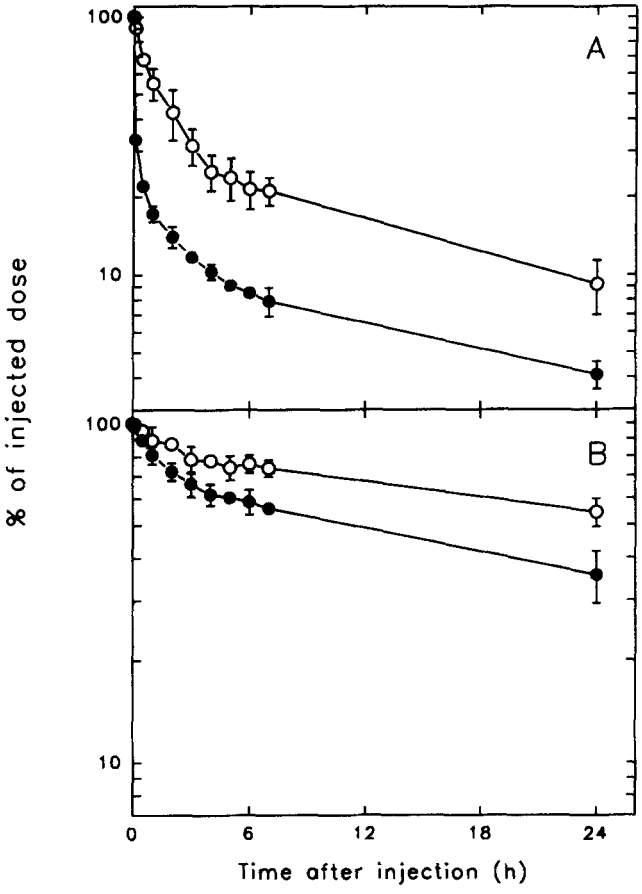

Fig. 1. Blood clearance curves of intravenously injected β-VLDL and LDL(cr) into cholesterol- and chow-fed rabbits. Blood clearance curves for chow-fed control rabbits (panel A) and cholesterol-fed rabbits (panel B) of intravenously injected ^{131}I-labeled TC-β-VLDL (closed circles) and ^{125}I-labeled TC-LDL(cr) (open circles) (n = 6). Data are shown as means ± SD.

TABLE 1. Plasma clearance parameters for β-VLDL and LDL(cr) in cholesterol-fed and control-fed rabbits

Parameter	Control-Fed Rabbits	Cholesterol-Fed Rabbits
FCR β-VLDL	1.58 ± 0.18	0.56 ± 0.08
ACR β-VLDL		25.3 ± 3.8
$T_{1/2}$ β-VLDL	10.7 ± 1.3	30.3 ± 4.6
FCR LDL(cr)	1.18 ± 0.12	0.42 ± 0.11
ACR LDL(cr)	6.73 ± 0.67	31.6 ± 8.1
$T_{1/2}$ LDL(cr)	14.2 ± 1.5	42.5 ± 10.4

The fractional catabolic rates (FCR) are expressed in plasma pools per day, the $T_{1/2}$s in hours, and the absolute catabolic rates (ACR) are expressed as mg apolipoprotein per day per kg rabbit (n = 6 for each group).

Hepatic uptake of β-VLDL is reduced in cholesterol-fed rabbits

As shown in **Fig. 2,** the hepatic uptake of ^{131}I-labeled TC-β-VLDL after 24 h as percent of injected dose was 26.6 ± 7.5% in control-fed rabbits as compared to 15.8 ± 6.7% in the cholesterol-fed rabbits (n = 6 in each group; $P < 0.05$). The uptake of ^{125}I-labeled TC-LDL(cr) was reduced by 75% after cholesterol feeding (n = 6 in each group; $P < 0.005$). However, considering the high plasma levels of lipoproteins in the cholesterol-fed rabbits, the absolute uptake of LDL(cr) was about 4-fold higher than that observed in the control animals; hepatic uptake of β-VLDL was 10 times higher than that of the controls.

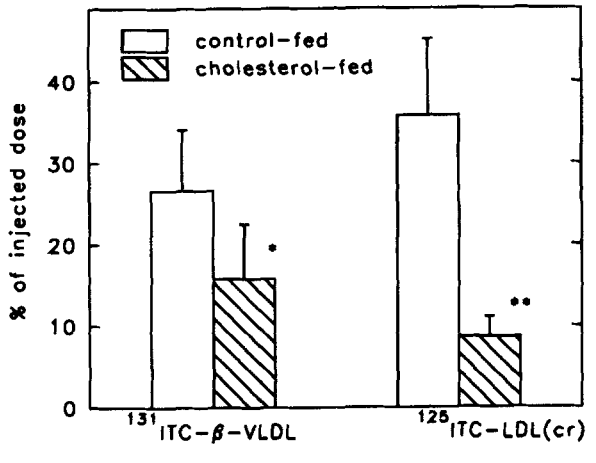

Fig. 2. Hepatic uptake of ^{131}I-labeled TC-β-VLDL and ^{125}I-labeled TC-LDL(cr) in cholesterol- and control-fed rabbits. The hepatic uptake of intravenously injected ^{131}I-labeled TC-β-VLDL and ^{125}I-labeled TC-LDL(cr) as percent of injected dose in cholesterol-fed rabbits (hatched bars) and chow-fed controls (open bars) are shown as mean ± SD; *,$P < 0.027$ (n = 6) vs. control, **,$P < 0.005$ (n = 6) vs. control.

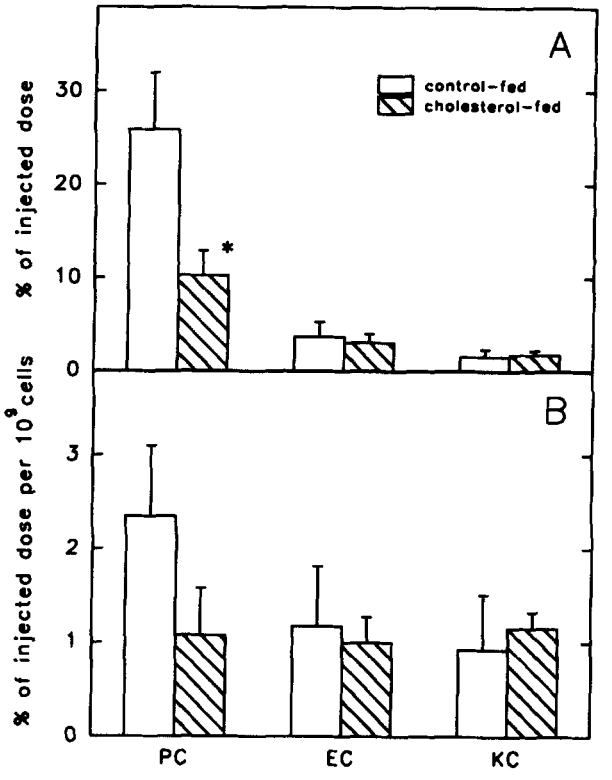

Fig. 3. Uptake of intravenously injected ^{131}I-labeled TC-β-VLDL in liver parenchymal, endothelial, and Kupffer cells. In vivo uptake of ^{131}I-labeled TC-β-VLDL in liver parenchymal (PC), endothelial (EC), and Kupffer cells (KC) 24 h after the injection are shown in cholesterol-fed (hatched bars) and control-fed rabbits (open bars) expressed as percent of injected dose in panel A and as percent of injected dose per 10^9 cells in panel B (mean ± SD); *,$P < 0.037$.

Distribution of injected β-VLDL in liver cells is altered after cholesterol feeding

The uptake of ^{131}I-labeled TC-β-VLDL as percent of injected dose in parenchymal, endothelial, and Kupffer cells is shown in **Fig. 3A.** Cholesterol feeding led to a reduced uptake of ^{131}I-labeled TC-β-VLDL in parenchymal liver cells, whereas the uptake of the lipoprotein in nonparenchymal liver cells was unaffected by cholesterol feeding. Thus, the relative distribution of ^{131}I-labeled TC-β-VLDL between the cells is altered after cholesterol feeding as shown in **Table 2.** In the cholesterol-fed animals, the parenchymal, Kupffer, and

TABLE 2. Distribution of β-VLDL taken up by different liver cell types in control and cholesterol-fed rabbits

Liver Cell Types	Control-Fed Rabbits	Cholesterol-Fed Rabbits
PC	83.9 ± 4.3	67.8 ± 8.7[a]
EC	11.4 ± 2.7	20.2 ± 5.3
KC	4.8 ± 1.7	12.1 ± 4.1[a]

The results are shown as percent of total hepatic uptake ± SD; PC, parenchymal cells; EC, endothelial cells; KC, Kupffer cells.
[a] $P < 0.03$ compared to control rabbits.

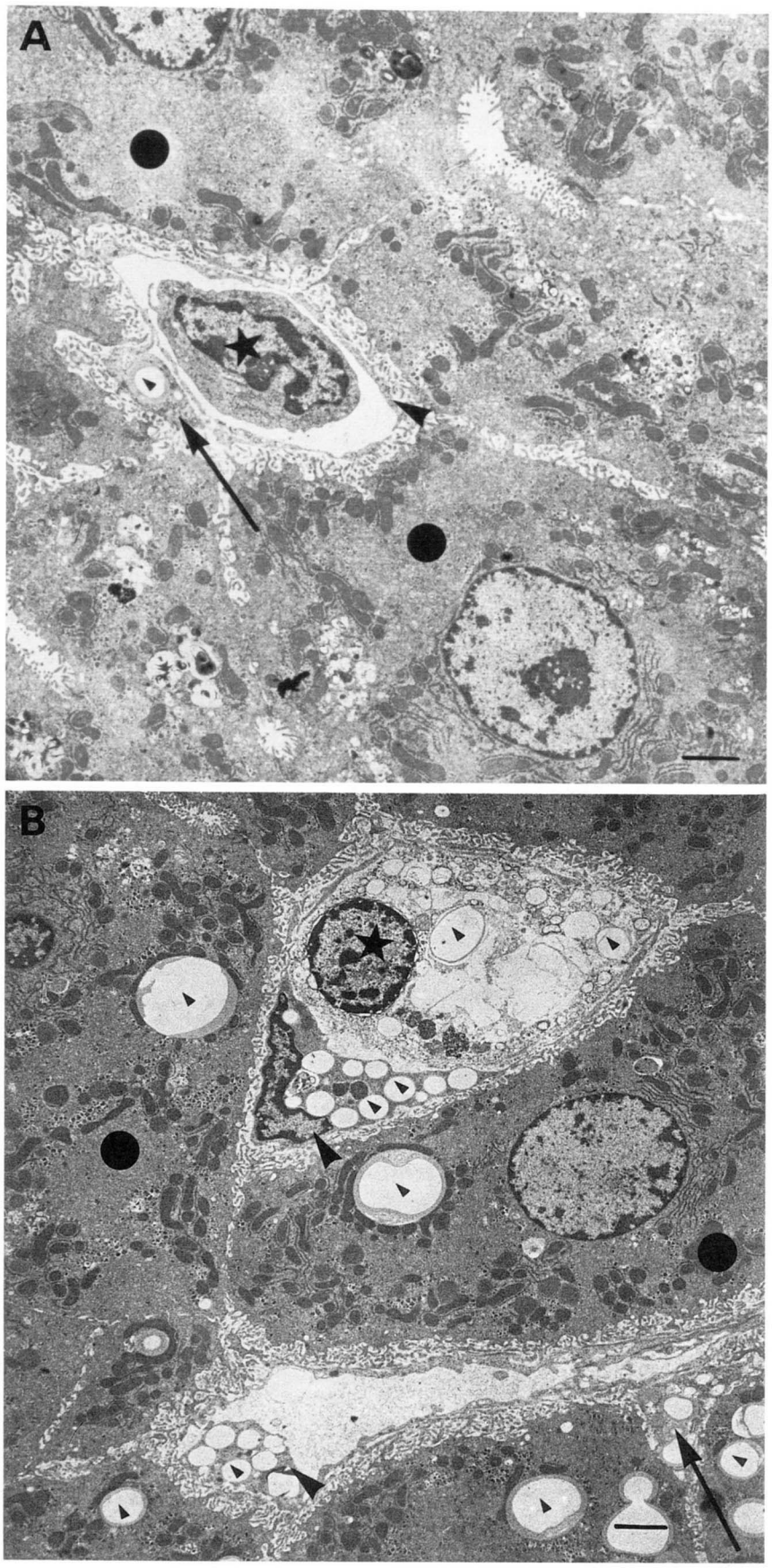

Fig. 4. Morphology in situ of different liver cell types in cholesterol-fed and chow-fed control rabbits. Appearance of different rabbit liver cell types in control (panel A) and in cholesterol-fed (panel B) animals in situ. Black dots label parenchymal cells, stars label Kupffer cells, arrows label stellate cells, and large arrow-heads label the endothelial lining. Small arrow-heads label lipid droplets. Bar represents 2 μm.

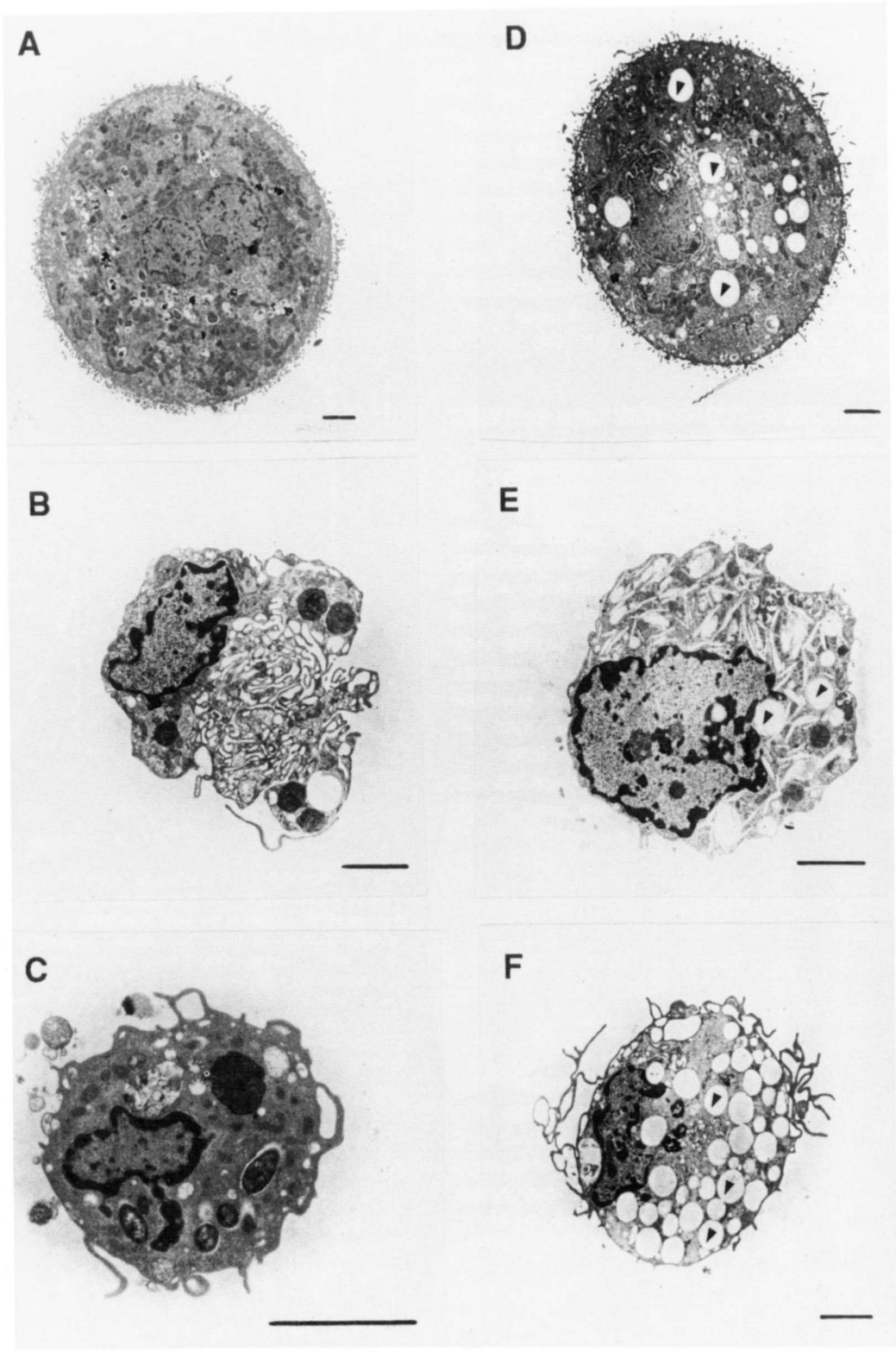

Fig. 5. Morphology of cultured liver cell types from cholesterol-fed and chow-fed control rabbits. Appearance of different isolated rabbit liver cell types from control (panels A–C) and cholesterol-fed (panels D–F) rabbits. Panels A and D depict parenchymal cells, panels B and E endothelial cells, and panels C and F Kupffer cells from control and cholesterol-fed animals, respectively. Small arrow-heads label lipid droplets. Bar represents 2 μm.

endothelial cells took up equal amounts of ^{131}I-labeled TC-β-VLDL per cell (Fig. 3B). In control animals, the parenchymal cells took up more than twice as much ^{131}I-labeled TC-β-VLDL as the Kupffer or endothelial cells on a per cell basis. On the other hand, the absolute uptake of β-VLDL was greatly increased in all cell types. In parenchymal cells the absolute uptake in the cholesterol-fed rabbits was 10-fold higher, in the endothelial cells it was 17-fold higher, and in Kupffer cells it was 30-fold higher than that of control rabbits. The nonparenchymal liver cells, notably the Kupffer cells, therefore, play an important role in blood clearance of β-VLDL in the cholesterol-fed rabbits.

Electron microscopic studies revealed large quantities of fat stored in all liver cell types

The rabbit liver morphology as seen in ultrathin, post-stain sections shows the arrangement of each liver cell type (**Fig. 4**). The ultrastructure is preserved after cholesterol feeding and corresponds to the description given in the introduction. All parenchymal liver cells in the cholesterol-fed rabbits contained very large lipid droplets (seen as "empty vacuoles"); some Kupffer cells contained many, other a few, and some no lipid droplets, whereas all the endothelial cells displayed large numbers of lipid droplets. Except for stellate cells, no other cell type displayed lipid droplets in control-fed rabbits.

In cultured cells from control and cholesterol-fed rabbits the same features as described above were seen (**Fig. 5**). Parenchymal cells contained numerous mitochondria, rough endoplasmic reticulum, an uneven nucleus, and had an almost round outline with numerous short microvilli. Parenchymal cells from cholesterol-fed rabbits displayed numerous large lipid droplets, while in control cells no such droplets could be observed. In sections from cultured endothelial cells, the fenestrated sieve plates and the thin cytoplasmic extensions that normally surround the sinusoid are seen as a mesh of numerous small spots in the cytoplasm. Large amounts of lipid droplets were seen in endothelial cells from cholesterol-fed rabbits. The cultured Kupffer cells contained various numbers of lipid droplets, confirming the in situ observations. The lipid droplets found in all liver cell types from the cholesterol-fed rabbits consist predominantly of cholesteryl esters (17).

Effect of cholesterol feeding on in vitro cell association of β-VLDL in rabbit parenchymal cells

Binding studies of β-VLDL in isolated parenchymal cells indicated that the binding could be divided into a saturable and an unspecific component (**Fig. 6 A,B**) (34). Transforming these data into a Scatchard plot revealed K_d values of 14.7 ± 14.0 μg/ml and 33.3 ± 9.3 μg/ml in cells from cholesterol-fed rabbits and chow-fed controls, respectively. The nonspecific binding was higher in the cholesterol-fed animals.

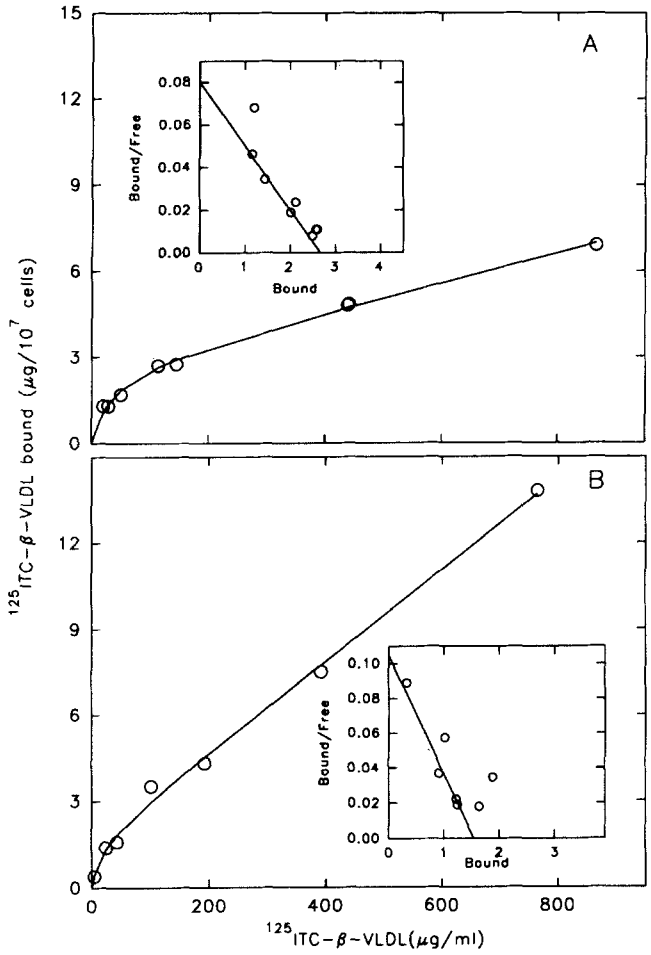

Fig. 6. Binding of ^{125}I-labeled TC-β-VLDL to liver parenchymal cells isolated from control chow-fed rabbits (panel A) and cholesterol-fed rabbits (panel B). The curves were best-fitted to a formula describing one specific binding site plus a nonspecific component: bound = Cap*free/(K_d + free) + nonsp. *free. Using this curve-fit the capacity (Cap), K_d, and the nonspecific component (nonsp.) were calculated. The dependencies for the K_d values were 0.80 in A and 0.70 in B. Specific bound ^{125}I-labeled TC-β-VLDL was calculated by subtracting the nonspecific component from the bound ligand (t = bound − nonsp.*free) and transformed: f(t) = $-t/K_d$ + Cap/K_d.

To study the specificity of β-VLDL binding and uptake in rabbit liver parenchymal cells, suspensions of isolated cells were incubated with labeled β-VLDL in the presence or absence of unlabeled control rabbit LDL, LDL(cr), human LDL, and β-VLDL. Incubations were done at 4°C (**Fig. 7 A,B**) and at 37°C (Fig. 7 C,D). The results obtained in control cells and in cells from cholesterol-fed rabbits were similar, although a higher nonspecific binding again was observed in cells from cholesterol-fed rabbits. Thus, the uptake of ^{125}I-labeled TC-β-VLDL at 37°C was nearly abolished by an approximately 100-fold excess of unlabeled β-VLDL in control cells, whereas a similar excess of β-VLDL reduced cell association about 80% in cells from cholesterol-fed rabbits (Fig. 7 C,D). Rabbit LDL (both LDL(cr) and control LDL) also

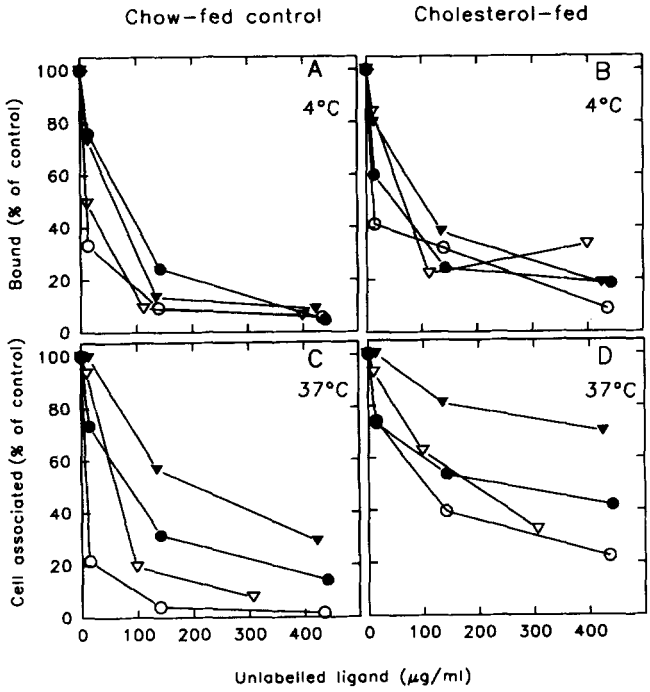

Fig. 7. Competition of different lipoproteins on cell association of ^{125}I-labeled TC-β-VLDL to suspended hepatocytes from cholesterol-fed and chow-fed rabbits. The figure shows competition studies of human LDL (closed triangles), control-rabbit LDL (closed circles), cholesterol-fed rabbit LDL (open triangles), and β-VLDL (open circles) on binding of ^{125}I-labeled TC-β-VLDL (5 μg/ml) at 4°C (panels A, B) and cell association of ^{125}I-labeled TC-β-VLDL at 37°C (panels C, D) to suspended parenchymal liver cells from chow-fed (panels A, C) and cholesterol-fed (panels B, D) rabbits.

efficiently reduced cell association of β-VLDL, whereas human LDL was a less effective competitor. The results obtained at 4°C deviated in some respects from those found at 37°C. Binding of ^{125}I-labeled TC-β-VLDL was inhibited to about the same extent by all lipoproteins tested (Fig. 7 A,B). However, a progressive reduction of ^{125}I-labeled TC-β-VLDL cell association was observed by unlabeled human LDL, control rabbit and cholesterol-fed rabbit LDL. Unlabeled β-VLDL was the most effective inhibitor of cell association.

DISCUSSION

The purpose of the present study was to determine the contribution of the different liver cell types to the hepatic uptake of β-VLDL in hypercholesterolemic rabbits. Previous studies in our laboratory have demonstrated that the nonparenchymal liver cells acquire a more important role in the hepatic uptake of LDL in cholesterol-fed rabbits than in control animals (15, 17). Negligible amounts of LDL(cr) were taken up in Kupffer or endothelial cells in control rabbits. In cholesterol-fed rabbits, on the other hand, the nonparenchymal liver cells, notably the endothelial cells, were of significant importance in the hepatic uptake of LDL(cr) accounting for more than 30% of the hepatic uptake (17). The present study demonstrates that the nonparenchymal liver cells assume a prominent role in the hepatic uptake of β-VLDL in hypercholesterolemic rabbits. In contrast to the hepatic distribution of injected LDL(cr), which showed a 4-fold rise in endothelial cells (17), the increased β-VLDL uptake in the nonparenchymal cells was most pronounced in the Kupffer cells (Table 2). Recently de Rijke, Hessels, and Van Berkel (35) published that oxidatively modified β-VLDL is recognized by binding sites on Kupffer cells in rats, while "less modified" lipoproteins such as acetylated LDL bind primarily to specific recognition sites on the rat liver endothelial cells (36, 37). Indications of in vivo modification of LDL and β-VLDL have been published (38, 39) [also discussed in recent reviews (40–44)]. Thus, one possible explanation for the increased uptake of β-VLDL in the Kupffer cells in the cholesterol-fed rabbits is that β-VLDL might have undergone oxidative modifications due to the long half-life in plasma. As the percent of hepatic β-VLDL catabolized by the Kupffer cells is more than doubled in hypercholesterolemic rabbits, one might suggest that β-VLDL becomes more "severely" modified in the cholesterol-fed rabbits than LDL(cr) although LDL(cr) has a longer half-life. Experiments are under way to describe the lipoprotein modifications induced by cholesterol feeding.

Particle size measurements showed that the diameters of β-VLDL and LDL(cr) were 60 nm and 30 nm, respectively. We do not know whether the larger size of β-VLDL compared to LDL(cr) may explain the high uptake of β-VLDL in the phagocytic Kupffer cells. Tabas and coworkers (45) found that β-VLDL particles were not phagocytosed in mouse peritoneal macrophages.

The FCR of β-VLDL was reduced in hypercholesterolemic rabbits, but considering the high plasma level of β-VLDL the absolute amount taken up by the parenchymal liver cells was increased. These cells contained large lipid droplets as seen in the electron microscope both in cells in culture and in situ (Figs. 4 and 5). The K_d value for the β-VLDL binding site on parenchymal cells isolated from hypercholesterolemic rabbits was measured to be less than 50 μg/ml. If the in vivo K_d is similar, the concentration of endogenous β-VLDL will exceed the K_d by a factor of nearly 100. The specific binding mechanism would then be saturated, leaving nonspecific mechanisms to dominate the uptake in hypercholesterolemic rabbits. One such nonspecific mechanism that could dominate the uptake at concentrations above saturation is fluid-phase endocytosis, because uptake by fluid-phase endocytosis is proportional to the concentration of solute taken up. We have found that Kupffer cells take up 5 times more fluid by fluid-phase endocytosis than liver endothelial cells (Gudmundsen, O., T. Gjøen, and T. Berg, unpublished

results). The plasma level of β-VLDL is increased relatively more above the saturation level than LDL(cr), and the Kupffer cells may therefore take up considerable amounts of β-VLDL by fluid-phase endocytosis in the hypercholesterolemic rabbits.

In accordance with findings by Kovanen and coworkers (10), our data show that β-VLDL in chow-fed rabbits is rapidly cleared from the plasma. We found that 5 min after injection approximately 33% of the injected dose could be recovered in the blood. Most of this rapidly cleared β-VLDL is presumably taken up by the liver as shown in dogs (9), rats (8), and in rabbits (10). The uptake of β-VLDL (26.6% of injected dose) observed in the livers of control animals after 24 h is relatively low. A much higher recovery would be expected if the liver is the main organ for uptake of β-VLDL.

The hepatic uptake may, however, be underestimated in both animal groups because of leakage of labeled tyramine cellobiose to the bile after protein degradation. Pittman and colleagues (22) found this leakage to be approximately 20% per 24 h after uptake of TC-labeled asialofetuin. As this leakage originates exclusively from the parenchymal liver cells, the results show an underestimation of the uptake in these cells and not in the nonparenchymal cells. The underestimation is probably smaller in the cholesterol-fed rabbits because the clearance was slow and the hepatic uptake of labeled β-VLDL was relatively low.

A rapid initial clearance was not observed in cholesterol-fed rabbits. After 5 min, 90% of the injected dose of β-VLDL was recovered in blood in these animals, indicating that the mechanism mediating the rapid initial uptake was down-regulated in the cholesterol-fed rabbits. A down-regulation of the specific uptake mechanism for β-VLDL was also measured in vitro in isolated parenchymal cells from cholesterol-fed rabbits. These cells showed a 40% reduction in uptake capacity as compared to controls. A specific apoE receptor on liver parenchymal cells has been postulated as a lipoprotein receptor for chylomicron remnants and other apoE-enriched lipoproteins. Our data, obtained in in vitro experiments with unlabeled ligands (Figs. 6 and 7), suggest that the only specific mechanism involved in the uptake of β-VLDL in both cholesterol-fed and chow-fed rabbits is the apoB,E receptor. This is in contrast to the findings in rats (8, 13), where β-VLDL is taken up by mechanisms independent of the apoB,E receptor in the liver. The apoB,E receptor has a higher affinity for apoE than for apoB and this affinity difference may explain differences in the hepatic uptake of LDL(cr) compared to β-VLDL in cholesterol-fed rabbits as well as the absence of a rapid initial clearance of LDL(cr) in control rabbits.

The in vitro data show an increased unspecific binding of β-VLDL after cholesterol feeding. This is in contrast to prior in vivo studies in our laboratory, in which no higher nonspecific component of LDL binding was observed in cholesterol-fed rabbits compared to controls using methylated LDL as a marker for nonspecific binding (15). One would expect the lipid-loaded parenchymal cells, as shown in the electron microscopical pictures, to have altered membrane properties. This may in turn influence the nonspecific binding of β-VLDL. The 40% loss in specific receptor capacity observed in the parenchymal cells from hypercholesterolemic rabbits in vitro would also contribute to nonspecific binding, because this will lead to a sustained higher concentration of β-VLDL.

In summary, our data show that the nonparenchymal cells, notably the Kupffer cells, play a more important physiological role in catabolizing β-VLDL in hypercholesterolemic rabbits than in chow-fed controls. In the control rabbits β-VLDL is taken up almost exclusively by the liver parenchymal cells. In vitro data suggest that the specific receptor involved in the uptake of β-VLDL in the liver parenchymal cells of both chow-fed and cholesterol-fed rabbits is the apoB,E receptor.

This study was supported by The Norwegian Council on Cardiovascular Disease, Blix Foundation, and The Norwegian Council of Science. We thank Vivi Volden, Kari Holte, Tove Bakar, and Anne Randi Alvestad for expert technical assistance, and Tom Berland, Rensheng Dou, and Torstein Jøssang for their help in determining lipoprotein particle sizes by light scattering.

Manuscript received 7 July 1992 and in revised form 16 October 1992.

REFERENCES

1. Havel, R. J., and P. J. Kane. 1973. Primary dysbetalipoproteinemia: predominance of a specific apoprotein species in triglyceride-rich lipoproteins. *Proc. Natl. Acad. Sci. USA.* **70:** 2015–2019.
2. Fainaru, M., R. W. Mahley, R. L. Hamilton, and T. L. Innerarity. 1982. Structural and metabolic heterogeneity of β-very low density lipoproteins from cholesterol-fed dogs and from humans with Type III hyperlipoproteinemia. *J. Lipid Res.* **23:** 702–714.
3. Goldstein, J. L., Y. K. Ho, M. S. Brown, T. L. Innerarity, and R. W. Mahley. 1980. Cholesterol ester accumulation in macrophages resulting from receptor-mediated uptake and degradation of hypercholesterolemic canine β-very low density lipoproteins. *J. Biol. Chem.* **255:** 1839–1848.
4. Territo, M. C., J. A. Berliner, L. Almanda, R. Ramirez, and A. M. Fogelman. 1989. β-Very low density lipoprotein pretreatment of endothelial monolayers increase monocyte adhesion. *Arteriosclerosis.* **9:** 824–828.
5. Daugherty, A., L. G. Lange, B. E. Sobel, and G. Schonfeld. 1985. Aortic accumulation and plasma clearance of β-VLDL and HDL: effects of diet-induced hypercholesterolemia in rabbits. *J. Lipid Res.* **26:** 955–963.
6. Pitas, R. E., T. L. Innerarity, and R. W. Mahley. 1983. Foam cells in explants of atherosclerotic rabbit aortas have receptors for β-very low density lipoproteins and modified low density lipoproteins. *Arteriosclerosis.* **3:** 2–12.
7. Daugherty, A., S. R. Thorpe, L. G. Lange, B. E. Sobel, and

G. Schonfeld. 1985. Loci of catabolism of β-very low density lipoprotein in vivo delineated with residualizing label, ^{125}I-dilactitol tyramine. *J. Biol. Chem.* **260:** 14564–14570.
8. Harkes, L., A. Duijne, and T. J. C. Van Berkel. 1989. Interaction of β-very-low-density lipoproteins with rat liver cells. *Eur. J. Biochem.* **180:** 241–248.
9. Fainaru, M., H. Funke, J. K. Boyles, E. H. Ludwig, T. L. Innerarity, and R. W. Mahley. 1988. Metabolism of canine β-very low density lipoproteins in normal and cholesterol-fed dogs. *Arteriosclerosis.* **8:** 130–139.
10. Kovanen, P. T., M. S. Brown, S. K. Basu, D. W. Bilheimer, and J. L. Goldstein. 1981. Saturation and suppression of hepatic lipoprotein receptors: a mechanism for the hypercholesterolemia of cholesterol-fed rabbits. *Proc. Natl. Acad. Sci. USA.* **78:** 1396–1400.
11. Naito, M., and E. Wisse. 1978. Filtration effect of endothelial fenestrations on chylomicron transport in the neonatal rat liver. *Cell Tissue Res.* **190:** 371–382.
12. Koo, C., M. E. Wernette-Hammond, Z. Garcia, M. J. Malloy, R. Uauy, C. East, D. W. Bilheimer, R. W. Mahley, and T. L. Innerarity. 1988. Uptake of cholesterol-rich remnant lipoproteins by human monocyte-derived macrophages is mediated by low density lipoprotein receptors. *J. Clin. Invest.* **81:** 1322–1340.
13. De Water, R., J. A. A. M. Kamps, M. C. M. Van Dijk, E. A. M. J. Hessels, J. Kuiper, J. K. Kruijt, and T. J. C. Van Berkel. 1992. Characterization of the low-density-lipoprotein receptor-independent interaction of β-very-low density lipoprotein with rat and human parenchymal liver cells. *Biochem. J.* **282:** 41–48.
14. Nenseter, M. S., O. Myklebost, R. Blomhoff, C. A. Drevon, A. Nilsson, K. R. Norum, and T. Berg. 1989. Low-density-lipoprotein receptors in different rabbit liver cells. *Biochem. J.* **261:** 587–593.
15. Nenseter, M. S., R. Blomhoff, C. A. Drevon, G. M. Kindberg, K. R. Norum, and T. Berg. 1988. Uptake of LDL in parenchymal and nonparenchymal rabbit liver cells in vivo. *Biochem. J.* **254:** 443–448.
16. Russell, D. W., M. S. Brown, and J. L. Goldstein. 1989. Different combinations of cysteine-rich repeats mediate binding of low density lipoprotein receptor to two different proteins. *J. Biol. Chem.* **264:** 21682–21688.
17. Nenseter, M. S., O. Gudmundsen, N. Roos, G. Mælandsmo, C. A. Drevon, and T. Berg. 1992. The role of liver endothelial and Kupffer cells in clearing low density lipoprotein from blood in hypercholesterolemic rabbits. *J. Lipid Res.* **33:** 867–877.
18. Folch, J., M. Lees, and G. H. Sloane Stanley. 1957. A simple method for the isolation and purification of total lipides from animal tissues. *J. Biol. Chem.* **226:** 497–509.
19. Laemmli, U. K. 1970. Cleavage of structural proteins during the assembly of the head of bacteriophage T4. *Nature.* **227:** 680–685.
20. Nenseter, M. S., R. Blomhoff, W. Eskild, G. M. Kindberg, and T. Berg. 1987. Intracellular transport and degradation of chylomicron remnants in rat liver cells after in vivo endocytosis. *Biochim. Biophys. Acta.* **929:** 25–33.
21. Havel, R. J., H. A. Eder, and J. H. Bragdon. 1955. The distribution and chemical composition of ultracentrifugally separated lipoproteins in human serum. *J. Clin. Invest.* **34:** 1345–1353.
22. Pittman, R. C., T. E. Carew, C. K. Glass, S. R. Green, C. A. Taylor, and A. D. Attie. 1983. A radioiodinated, intracellularly trapped ligand for determining the sites of plasma protein degradation in vivo. *Biochem. J.* **212:** 791–800.
23. Pecora, R. 1985. Dynamic Light Scattering. Applications of Photon Correlation Spectroscopy. Plenum Press, New York.
24. Ross, A. C., and D. B. Zilversmit. 1977. Chylomicron remnant cholesteryl esters as the major constituent of very low density lipoproteins in plasma of cholesterol-fed rabbits. *J. Lipid Res.* **18:** 169–181.
25. Matthews, C. M. E. 1957. The theory of tracer experiments with ^{131}I-labelled plasma proteins. *Phys. Med. Biol.* **2:** 36–53.
26. Berry, M. N., and D. S. Friend. 1969. High-yield preparation of isolated rat liver parenchymal cells. *J. Cell Biol.* **43:** 506–520.
27. Seglen, P. O. 1976. Preparation of isolated rat liver cells. *Methods Cell Biol.* **13:** 29–83.
28. Berg, T., and R. Blomhoff. 1983. Preparation of isolated rat liver cells. *In* Iodinated Density Gradient Media—A Practical Approach. D. Rickwood, editor. IRL Press Limited, Oxford. 173–174.
29. Tolleshaug, H., T. Berg, M. Nilsson, and K. R. Norum. 1977. Uptake and degradation of ^{125}I-labelled asialo-fetuin by isolated rat hepatocytes. *Biochim. Biophys. Acta.* **499:** 73–84.
30. Laakso, T., and B. Smedsrød. 1987. Cellular distribution in rat liver of intravenously administered polyacryl starch and chondroitin sulfate microparticles. *Int. J. Pharm.* **36:** 253–262.
31. Munthe-Kaas, A. C., T. Berg, and R. Seljelid. 1976. Distribution of lysosomal enzymes in different types of rat liver cells. *Exp. Cell Res.* **99:** 146–154.
32. Blomhoff, R., K. Holte, L. Næss, and T. Berg. 1984. Newly administered [^{3}H]retinol is transferred from hepatocytes to stellate cells in liver for storage. *Exp. Cell Res.* **150:** 186–193.
33. Kindberg, G. M., O. Gudmundsen, and T. Berg. 1990. The effect of vanadate on receptor-mediated endocytosis of asialoorosomucoid in rat liver parenchymal cells. *J. Biol. Chem.* **265:** 8999–9005.
34. Munson, P. J., and D. Rodbard. 1980. LIGAND: a versatile computerized approach for characterization of ligand-binding systems. *Anal. Biochem.* **107:** 220–239.
35. De Rijke, Y. B., E. M. A. J. Hessels, and T. J. C. Van Berkel. 1992. Recognition sites on rat liver cells for oxidatively modified β-very low density lipoproteins. *Arterioscler. Thromb.* **12:** 41–49.
36. Van Berkel, T. J. C., Y. B. De Rijke, and J. K. Kruijt. 1991. Different fate in vivo of oxidatively modified low density lipoprotein and acetylated low density lipoprotein in rats. Recognition by various scavenger receptors on Kupffer and endothelial liver cells. *J. Biol. Chem.* **266:** 2282–2289.
37. Blomhoff, R., C. A. Drevon, W. Eskild, P. Helgerud, K. R. Norum, and T. Berg. 1984. Clearance of acetyl low density lipoprotein by rat liver endothelial cells. *J. Biol. Chem.* **259:** 8898–8903.
38. Parthasarathy, S., M. T. Quinn, D. C. Schwenke, T. E. Carew, and D. Steinberg. 1989. Oxidative modification of beta-very low density lipoprotein. *Arteriosclerosis.* **9:** 398–404.
39. Palinski, W., M. E. Rosenfeld, S. Ylä-Herttuala, G. C. Gurtner, S. S. Socher, S. W. Butler, S. Parthasarathy, T. E. Carew, D. Steinberg, and J. L. Witztum. 1989. Low density lipoprotein undergoes oxidative modification in vivo. *Proc. Natl. Acad. Sci. USA.* **86:** 1372–1376.
40. Witztum, J. L. 1991. The role of oxidized LDL in atherosclerosis. *Adv. Exp. Med. Biol.* **285:** 353–365.
41. Witztum, J. L., and D. Steinberg. 1991. Role of oxidized

low density lipoprotein in atherogenesis. *J. Clin. Invest.* **88:** 1785–1792.
42. Steinberg, D. 1991. Antioxidants and atherosclerosis. *Circulation.* **84:** 1420–1425.
43. Rosenfeld, M. E. 1991. Oxidized LDL affects multiple atherogenic cellular responses. *Circulation.* **83:** 2137–2140.
44. Ylä-Herttuala, S. 1991. Macrophages and oxidized low density lipoproteins in the pathogenesis of atherosclerosis. *Ann. Med.* **23:** 561–567.
45. Tabas, I., J. N. Myers, T. L. Innerarity, X. X. Xu, K. Arnold, J. Boyles, and F. R. Maxfield. 1991. The influence of particle size and multiple apoprotein E-receptor interactions on endocytic targeting of β-VLDL in mouse peritoneal macrophages. *J. Cell Biol.* **115:** 1547–1560.